Expanded Tunability of Dynamic Hydrogel Stiffness Using Engineered Photoresponsive Proteins

Rossana Scavone

A thesis

submitted in partial fulfillment of the

Master of Science in Chemical Engineering

University of Washington

2019

Committee

Cole A. DeForest, chair

François Baneyx

Program Authorized to Offer Dregee:

Chemical Engineering

University of Washington

Abstract

Expanded Tunability of Dynamic Hydrogel Stiffness Using Engineered Photoresponsive Proteins

Rossana Scavone

Chair of the Supervisory Committee
Assistant Professor Cole A. DeForest

The extracellular matrix (ECM) plays an important role in regulating cell fate and function through dynamic and heterogenous presentation of well-defined chemical and mechanical cues. Though several research efforts have been focused on trying to elucidate the effects of ECM-mediated cues on cell function, few *in vitro* platforms have been able to capture the four-dimensionality of mechanical signaling that is presented *in vivo*. Towards this, our group recently introduced a hydrogel platform that undergoes reversible stiffening, made possible using a fusion protein-based material crosslinker that underwent a stimuli-dependent conformational change. The protein used was LOV2-Jα, a species that responds to mild visible light and gives spatiotemporal control on the hydrogel stiffness. In this work, we seek to expand the mechanical tunability of these protein-polymer-based hydrogels through well-defined mutations.

Contents

List of Figures

A Introduction

In every tissue, cells are supported by the extracellular matrix (ECM). The ECM is a three-dimensional network that not only provides structural support but also initiates biochemical and biomechanical cues that affect cell fate and function [1]. Cell functions including proliferation, differentiation, and migration are regulated by a series of soluble and mechanical cues present in the ECM [2]. For example, bone marrow mesenchymal stem cells (MSCs) differentiation process is modulated by ECM stiffness; MSCs in soft media undergo chondrogenic differentiation while those in stiff substrates grow into smooth muscle cells [3]. Another example is how the elastic modulus of the cell microenvironment affects muscle stem cell self-renewability [4]. Both examples show the importance of ECM biomechanical cues, more specifically the ECM stiffness, in governing cell fate. In recent years, research has been sought to investigate the specific mechanisms of ECM-mediated cellular regulations, but there are still shortcomings mainly due to the difficulty to imitate the ECM characteristics *in vitro*. The ECM is highly dynamic and its properties vary substantially from one tissue to another, but also throughout individual tissues and different physiological states (normal versus diseased) [1]. Brain and lung tissue have low average stiffness with a storage modulus of around 100 Pa, while bone or muscle have stiffness of several orders larger [5]. Also, every cell in the body is subjected to a cyclic force load associated with pulsatile blood flow from the circulatory system. Thus, cell culture platforms with dynamic mechanical properties that can be controlled by the user remain in great need.

Flat, static, and unphysiologically stiff materials have traditionally been used to conduct cell culture experiments. Although these materials are useful due to their simplicity, they present an aphysiological culture environment that can result in abnormal cell behavior

[6]. More recently, biomaterials research has focused on the development of platforms that better mimic *in vivo* characteristics. Among them, hydrogels represent a highly attractive option. Thanks to their high-water content, tissue-like elasticity, and easy transport of nutrients and waste, hydrogels have successfully been used for *in vitro* cell culture [7]. Furthermore, hydrogels are being modified to introduce properties that mimic the complexities found in native cell environments. Several platforms have been reported that are capable of responding to external or internal stimuli, changing its physiological state [8]. The effects on stiffness change in cell fate have been studied on stimuli-responsive hydrogels using light [9] [10] [11], voltage [12], pH [13] and temperature [14].

Among the list of external stimuli that can be used, light provides a powerful on/off regulation with unique spatial and temporal control [8]. Recently, our group created a material with reversible and cyclical stiffening by using a light-responsive protein as linker in a poly(ethylene glycol)-based hydrogel [15]. The fusion protein selected was the light, oxygen and voltage sensing domain 2 (LOV2), which is part of the photosensory domain of phototropins, one of the photoreceptors found in plants (Figure 1). LOV2 acts as a blue-light sensor thanks to its cofactor, the chromophore flavin mononucleotide (FMN). This cofactor is initially held to the binding pocket by hydrogen bonds and Van der Waals forces with several aminoacidic residues [16]. Upon light excitation in the region of 470 nm, a covalent thioether bond is formed between FMN and a conserved cysteine residue in LOV2 domains. Furthermore, this is accompanied by a conformational shift from the C terminal α helix structure known as Jα, which shifts away after the thioether bond is formed [17]. This process is also fully reversible, presenting a dark recovery to its ground state. When used as part of the hydrogel structure, the conformational change induced by light excitation results in a change on the material stiffness, achieving a softer state and recovering to the original stiffness once light exposure is ceased. The reported results not

only showed this feature but also demonstrate that the system was cyclable [15].

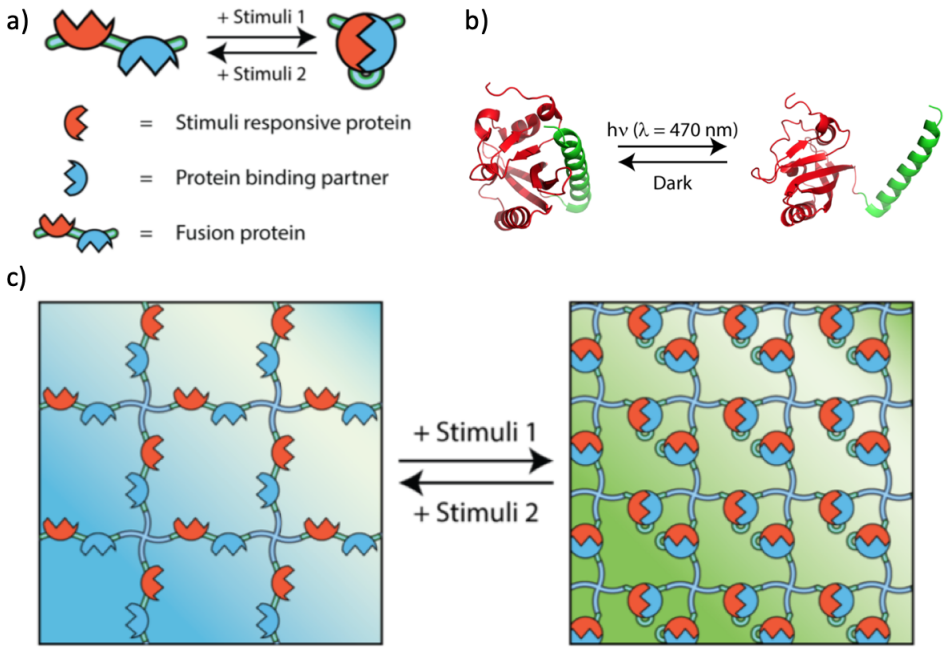

Figure 1: Fusion proteins as hydrogel crosslinkers.
a) Genetically-encoded fusion protein exhibits different conformations and end-to-end length in response to stimuli. b) Light, oxygen and voltage sensing domain 2 (LOV2, in red) and its binding partner Jα (in green). In response to blue light (470nm) Jα shifts away form LOV2; this change is reversible in the dark. c)When used as crosslinker in hydrogels, the fusion protein conformational change generates a reversible stimuli-dependent change in the material stiffness.

Though the cyclability and spatiotemporal control of the LOV2-based system represents a major step forward in the available platforms to study biomechanics, there is still substantial room for improvement. According to our previously reported data, though the softer state was reached almost instantaneously, the dynamics of the dark recovery showed a half-life of 35 s. This time frame could be too fast for studying healing processes (days) [18] or too slow compared to the pulsatile dynamics of the circulatory system (~1 second). Also, the largest observed difference in moduli from the stiff to the soft state was ~15%

[15], which is relatively small for many applications including tissue-specific fibrosis [19]. In this work, we sought to improve these shortcomings by modifying the photoresponsive characteristics of LOV2, namely the dynamics of its photocycle and the extent of Jα conformational shift.

B Methodology

B.1 Plasmid construction for LOV2 mutant genes

Plasmids containing each LOV2 mutation were constructed by different standard cloning techniques. STEPL plasmid containing the LOV2-Jα gene and ampicillin resistance [15] was used as the starting point for site-specific mutations. This gene also contained the recognition sequences for NMT at the N terminal (in this case MGNEASYPL) and sortase at the C terminal (in this case LPETG) for azido-functionalization, requisite to create protein-based material crosslinkers. A site-directed mutagenesis protocol was performed. This method uses PCR amplification, starting with primers that carry the mutation to be introduced in the gene. After PCR, the enzyme DpnI is used to eliminate the template plasmid, leaving the one carrying the mutation intact. For the mutant with the flexible spacers sequence, the gene for LOV2-$(G_4S)_3$- Jα was obtained in the form of a gBlock from Integrated DNA Technologies. The sequence included the flanking recognition sequences for azido-functionalization, two restriction enzyme sites at both ends (NdeI and XhoI) and two restriction enzyme sites flanking the spacer sequence (KpnI and BamHI). This gene sequence and the STEPL plasmid template were digested using NdeI and XhoI and then ligated together with T_4 DNA ligase. In both cases, the resulting plasmids were transformed into electrocompetent Top10 *E. Coli* by electrical shock using a BioRad micropulser (17 kV/cm), and plated onto agar plates (10 g Tryptone, 5 g Yeast Extract, 10 g NaCl, 15 g agar, 1 L dH2O) containing ampicillin (100 µg/mL). Colonies were selected according to antibiotic resistance, plasmid extracted, purified and sequenced to verify correct mutation.

B.2 Synthesis of LOV2 mutant proteins

Purified STEPL plasmids containing the mutants were co-transformed with NMT encoding plasmid (containing kanamycin resistance) in electrically competent BL21 *E. Coli* by electrical shock. Successful colonies were selected and grown at 37 ^{o}C in lysogeny broth. Culture growth was monitored by optical density (OD) measurements; when OD$_{\sim}$0.6, protein expression was induced by adding isopropyl β-D-1-thiogalactopyranoside (IPTG, 0.5mM) and 12 ADA (140 mg/L). The culture was then left to express the protein overnight at 18 ^{o}C. Bacteria cell pellets were centrifuged, resuspended and sonicated in a lysis buffer (20 mM Tris, 50 mM NaCl, 10 mM imidazole, 1 mM phenylmethylsulfonyl fluoride). The sonicated mixture was then centrifuged and the supernatant was added to 4 mL of Ni-NTA resin to bind for one hour at 4 ^{o}C. Then, conjugation buffer (20 mM Tris, 50 mM NaCl, 100 µM $CaCl_2$) was added containing the polyglycine peptide probe with the azido group (H-GGGGDDK(-N_3)-NH_2) and sortase reaction was carried for 4 hours at 37 ^{o}C. Finally, the protein was eluted, concentrated by centrifugation using a spin column (Amicon, cut off = 10 kDa molecular weight) and lyophilized.

B.3 Photocycle dynamics characterization

LOV2 dark recovery can be followed by measuring the UV-Vis absorbance spectra after light exposure [20]. In this case the analysis was performed using a NanoDrop spectrophotometer. The absorbance spectrum was measured over time. Additionally, the time dependence of absorbance at $\lambda = 450$ nm was fitted to an exponential function to determine the lifetime of the dark recovery for each mutant.

B.4 Rheology studies

Rheological experiments were run with an Anton Paar rheometer. The hydrogels were formed on the rheometer by mixing PEG-tetraBCN (3mM, ~20 kDa), linear PEG-diazide (3 mM, ~3.4 kDa) and the diazide-modified fusion protein (3 mM in STEPL buffer, 20 mM Tris, 50 mM NaCl, pH = 7.0), between parallel plates (8 mm diameter). A volume of 10 µL was used to form hydrogels with ~0.1 mm thickness. The storage and loss moduli (G' and G" respectively) were measured at constant strain (1%) and frequency (1 rad/s). The hydrogel was allowed to form for 4 hours while monitoring G' and G". Then, the light effect on stiffness was studied by exposing the gel to blue light source (λ = 470 nm, 5 mW/cm^2).

C Results and discussion

The photocycle of LOV2 can be affected by a number of different factors. Zayner *et.al* previously performed a mutational analysis on LOV2 to better understand its photocycle mechanism; they identified the residues that interact with the chromophore FMN and mutated them to inert residues [20]. Apart from the active-site cysteine C450, which is essential for LOV2 to carry the photocycle, the mutations permitted photocycling but changed its dynamics. Among the residues that were studied, we focused our efforts on three that showed interesting effects. Residues Q513 and N492 interact with FMN in LOV2 dark state. Mutations on these residues change the binding pocket nature and affect the photocycle lifetime. Other residues have a more indirect effect, like N414. This residue does not interact with FMN but controls water entry at the binding pocket. According to Zayner, water plays an important role in LOV2 dark recovery, catalyzing the proton transfer that in turn generates the breakage of the covalent bond between FMN and cysteine residue [20]. Mutating N414 to hydrophobic groups make the photocycle slower and hydrophilic groups make it faster. From the data reported in Zayner work, we selected three mutants: Q315L for longer photocycle and N414D and N492A for shorter photocycle (Figure 2).

The stiffness range that can be achieved in the LOV2-crosslinked gel system is related to the conformational shift that Jα undergoes after light exposure. This structure is connected to LOV2 by an unstructured aminoacidic sequence. We hypothesized that by varying the length of the connecting sequence, the overall extent of stiffness modulation could be tuned. To probe this, we genetically added a flexible aminoacidic sequence between LOV2 and Jα (Figure 2). The spacers sequence chosen consisted of four glycine and one serine, repeated three times $(G_4S)_3$. Since the unstructured region between LOV2 and Jα is not

conserved among different organisms that express this protein [21] we hypothesized that the introduction of spacers would not affect the ability of LOV2 to photocycle.

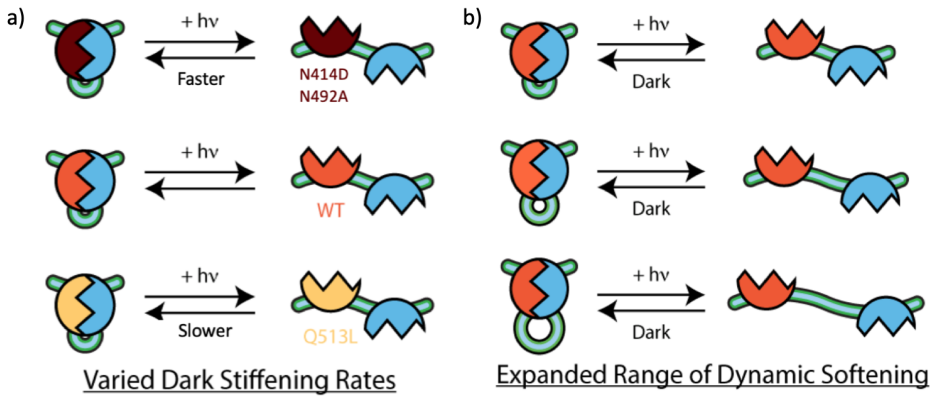

Figure 2: Fusion protein mutants and their effects.
a) Different mutants exhibit different photocycle dynamics. b)Flexible spacers sequence between LOV2 and Jα expand the range of stiffness in the material.

The hydrogels made in this work were based on the step-growth-polymerization between poly(ethylene glycol) (PEG)-tetrabicyclononyne (BCN) and a di-azide containing crosslinker. The network is formed by a strain-promoted azide-alkyne cycloaddition (SPAAC) reaction according to the procedure describe in DeForest *et.al* [22]. Here, a bicyclononyne reacts with an azido group to form a triazole linkage. The SPAAC reaction occurs between a four-arm poly(ethylene glycol)tetrabicyclononyne (PEGtetraBCN, Molecular Weight ~20 kDa), a linear PEG diazide (N_3-PEG-N_3, Molecular Weight ~3.4 kDa) and the different LOV2 mutants that are end-functionalized with azides groups (N_3). This reaction gives rise to idealized networks with well-defined stoichiometry and regularity. In order to add the reactive azido handles on the mutant proteins, two chemoenzymatic modifications were performed (Figure 3). N-terminal modification is done by the enzyme N-myristoyltransferase (NMT), which is a eukaryote enzyme that appends a fatty acid to the

N-terminal of protein with a certain recognition sequence [23]. Normally, the fatty acid used by the enzyme is myristic acid, but NMT's promiscuity allows it to covalently append analog species onto N-terminus. We exploit this promiscuity to ligate 12-azidododecanoic acid (12-ADA), thereby introducing azido functionality site-specifically onto the protein N-terminus. The C-terminal modification was achieved by the sortase-tag expressed protein ligation (STEPL) procedure [24] [25]. This method uses the enzyme Sortase A (Srt A) from *Staphylococcus aureus*, which is a calcium-assisted transpeptidase that recognized the motif LPXTG (where X is a random aminoacid) and binds to it a N-terminal polyglycine peptide/protein. Warden *et.al* created a single chimeric protein fusion that contains the protein to be modified, a flexible linker, Srt A and a His-tag. In this way, the conjugation can be done at the same time as purification by Ni-NTA chromatography. Using STEPL in conjunction with an azide-containing polyglycine peptide allows for quantitative functionalization of the C terminus with the reactive handle for gel formation.

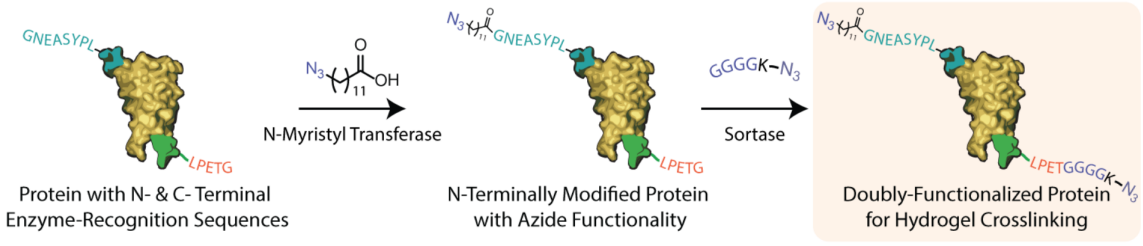

Figure 3: Functionalization of recombinant proteins for hydrogel incorporation. Proteins with the N-terminal GNEASYPL sequence are recognized by N-myristoyltransferase (NMT), which adds 12-azidododecanoic acid (12-ADA) to its N-terminal. Species containing the C-terminal LPETG sequence can be modified via a sortase-mediated transpeptidation with an azide-functionalized polyglycine probe. The final protein is end-functionalized with reactive azides, which are exploited to form hydrogel biomaterials via bioorthogonal SPAAC chemistry.

Different cloning techniques were performed to obtained plasmids coding for the different mutants. Site-directed mutagenesis was utilized for the mutants Q513L, N414D and

N492A. Alternatively, for the flexible spacer mutant, the whole gene coding for the protein was ligated to STEPL plasmid, using two restriction enzymes. It is important to note that the restriction enzyme used in the N-terminal, NdeI, introduces an ATG codon at the beginning of the protein gene, adding a methionine to the protein sequence as a cloning scar. Due to the effects this has on the performance of NMT in the modification of the N-terminal, a site-directed mutagenesis was performed to change this ATG for ATT. The gene sequences for each mutant can be found in the Appendix.

All the mutants were produced, with purified yields between 2-3 mg/L. Mass spectroscopy was performed to verify that the functionalization of both ends was achieved. The results are shown in Figure 4, showing that all the proteins were obtained with relatively high purity. Furthermore, the masses correlate to the expected values, verifying that all the mutants were correctly functionalized.

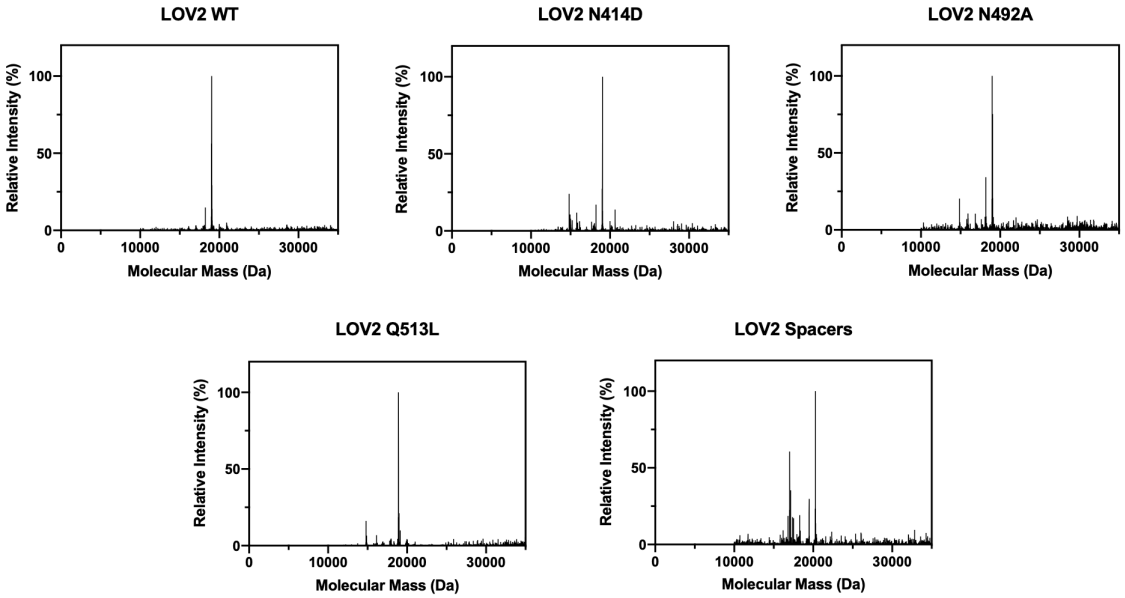

Figure 4: Mass Spectrometry data
Mass Spectrometry data for the un-mutated LOV2 (LOV2 WT) and for the four mutants obtained.

To further characterize the mutants, a photokinetic study was performed. The absorbance was monitored after blue light exposure (λ = 470 nm, 5 mW/cm^2 for 30 s). All the mutants showed the absorbance shift and the dark recovery characteristic of LOV2 (Figure 5), confirming that the protein is photoactive and FMN is present. Furthermore, the dynamics of the dark recovery were determined. For this, the absorbance data at 450 nm was fitted into an exponential decay function, and the half-life was calculated (Figure 6). The results showed that the mutants N492A and N414D have a faster dark recovery (6.6 $\pm$0.5 s and 7.9 $\pm$0.9 s respectively) while Q513L recovers slower (106 $\pm$2 s) than the wild type LOV2 (18.26 $\pm$0.98 s), as it was expected form previous studies [20]. Furthermore, the mutant with the flexible spacer sequence exhibits statistically indistinguishable photocycle dynamics (dark recovery half time of 22.6 $\pm$1 s) when compared with the unmutated

species. This was also expected since the spacers do not modify the binding pocket nor the way FMN interacts with LOV2.

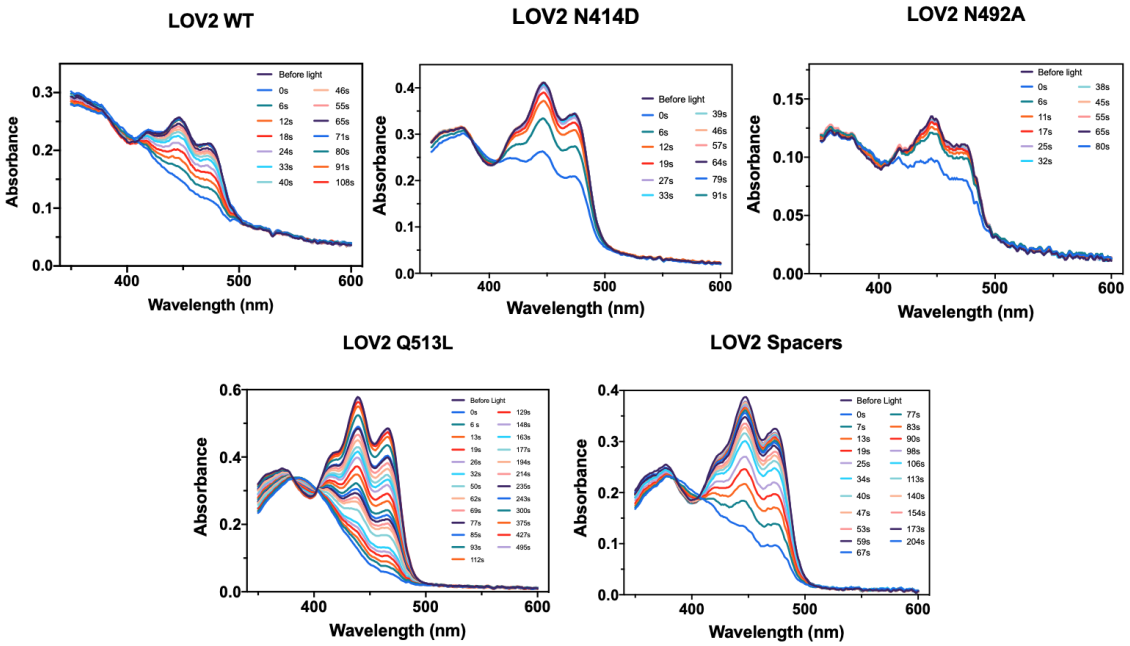

Figure 5: Absorbance spectrum for all LOV2 mutants

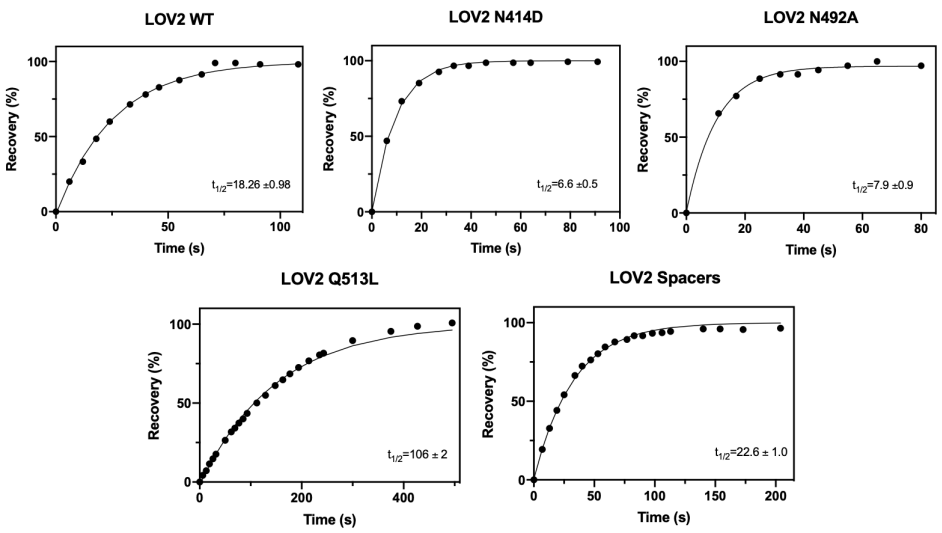

Figure 6: Exponential decay fitting to LOV2 dark recovery

Having demonstrated that all the mutants can be produced with high purity, are functionalized, and demonstrate the expected photoresponsive behavior; we sought to use these species as hydrogels crosslinkers. These were formed by mixing PEG-tetraBCN (3mM), linear PEG-diazide (3 mM) and the fusion protein (3 mM), meaning that the protein represents 50% of the crosslinking structure. The un-mutated LOV2 protein was studied first to recapitulate the results Liu *et.al* reported and to have as reference to compare with the other mutants results. Figure 7 shows the result for the first attempts. Hydrogels formed as expected, but when exposed to light, the hydrogel unexpectedly seemed to become stiffer, instead of reaching the softer state reported previously. This phenomenon was potentially explained by recent work from Lin lab, that demonstrated the photostiffening of hydrogels through an FMN-mediated tyrosine dimerization mechanism induced with 440 nm light exposure [26]. We hypothesize that the cofactor FMN is no longer bound from the LOV2 pocket and has become available to induce dimerization. The ineffective binding of FMN

could be caused by problems in the protein's purification processes.

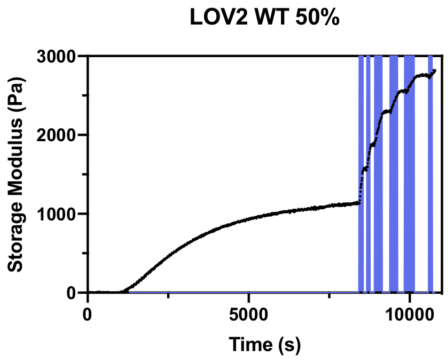

Figure 7: Stiffness increase in LOV2 hydrogels
When exposed to light (λ= 470 nm, 5 mW/cm^2, as indicated with blue bars), the hydrogel gets stiffer, potentially due to FMN-mediated tyrosine dimerization.

The study was conducted again with a fresh batch of the proteins. In this case, the wild type LOV2 (LOV2 WT) and the mutation containing the spacers sequences showed the expected behavior, as depicted in Figure 8. The data collected seems to have a great amount of noise, that could be due to the fact that the stiffness changes in this system are too small for the rheometer to accurately measure them. Despite that, a trend can be seen in the data, showing that in both cases the hydrogels does indeed become softer when exposed to light. Additionally, the change measured in the system using the wild type LOV2 had a smaller stiffness change than the one with the mutant containing the spacers, as it was expected (~2% change and ~5% change respectively). In the case of the mutant containing the spacers sequence, it should be noted that an increase on the overall hydrogel stiffness can be seen in each consecutive cycle. This could potentially be explained by the effect of tyrosine dimerization previously commented.

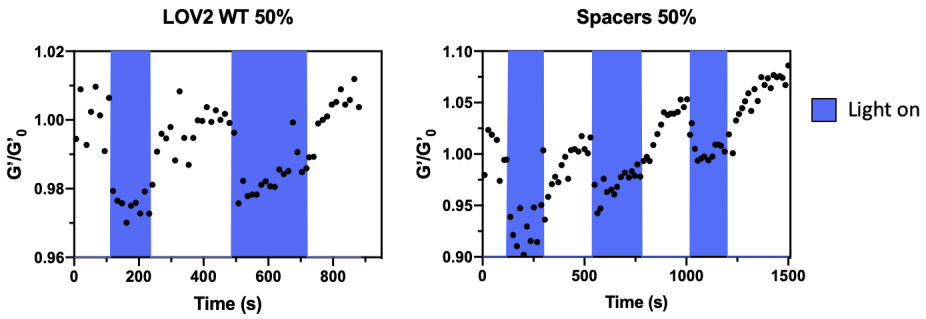

Figure 8: Rheological study of LOV2 hydrogels and the effect of light exposure on their stiffness

D Conclusion

The results presented in this work show how the mechanical tunability can be expanded by modifying the photoresponsive characteristics of the fusion LOV2-Jα. The effects of different well-defined site-specific mutations were studied, showing drastic changes in the dynamics of the photocycle for the protein in solution. Further work could be done to study the effects of the site-specific mutants on the dynamics of the stiffness change. Additionally, the introduction of a flexible spacer increased the stiffness change between the soft and stiff states of the hydrogels. We expect that utilization of spacer sequences of different lengths will further expand the dynamic range accessible using the LOV2-Jα system.

E Appendix

The DNA sequences for all the mutants are presented below, reading from 5' to 3'. A color code was used to identify the different components of the gene construct: The fusion protein is in black, with the mutation presented in blue. In green is the recognition sequence for NMT (RS1) and in orange the STEPL construct that includes the sortase recognition motif LPETG, a flexible linker $(GGS)_5$, the enzyme SrtA and a 6xHis tag.

RS1-LOV2(Q513L)-Jα-STEPL

ATGGGTAACGAAGCGTCTTACCCGCTGTTGGCTACTACACTTGAACGTATTGAGAAGAACTTT
GTCATTACTGACCCAAGATTGCCAGATAATCCCATTATATTCGCGTCCGATAGTTTCTTGCAGT
TGACAGAATATAGCCGTGAAGAAATTTTGGGAAGAAACTGCAGGTTTCTACAAGGTCCTGAAA
CTGATCGCGCGACAGTGAGAAAAATTAGAGATGCCATAGATAACCAAACAGAGGTCACTGTTC
AGCTGATTAATTATACAAAGAGTGGTAAAAAGTTCTGGAACCTCTTTCACTTGCAGCCTATGCG
AGATCAGAAGGGAGATGTCCAGTACTTTATTGGGGTTGATTTGGATGGAACTGAGCAT
GTCCGAGATGCTGCCGAGAGAGAGGGAGTCATGCTGATTAAGAAAACTGCAGAAAATATTGATG
AGGCGGCAAAAGAACTTCTCGAGCTGCCGGAAACCGGTGGTGGTAGTG
GTGGCTCTGGCGGTTCTGGTGGCAGTGGCGGTAGCCAAGCTAAACCTCAAATTCCGAAAGA
TAAATCAAAAGTGGCAGGCTATATTGAAATTCCAGATGCTGATATTAAAGAACCAGTATATCCAG
GACCAGCAACACCTGAACAATTAAATAGAGGTGTAAGCTTTGCAGAAGAAAATGAATCACTAGA
TGATCAAAATATTTCAATTGCAGGACACACTTTCATTGACCGTCCGAACTATCAATTTACAAATCT
TAAAGCAGCCAAAAAAGGTAGTATGGTGTACTTTAAAGTTGGTAATGAAACACGTAAGTATAAAAT
GACAAGTATAAGAGATGTTAAGCCAACAGATGTAGAAGTTCTAGATGAACAAAAAGGTAAAGATA
AACAATTAACATTAATTACTTGTGATGATTACAATGAAAAGACAGGCGTTTGGGAAAAACGTAAAA
TCTTTGTAGCTACAGAAGTCAAACATCACCACCATCATCACTAA

RS1-LOV2(N492A)-Jα-STEPL

ATGGGTAACGAAGCGTCTTACCCGCTGTTGGCTACTACACTTGAACGTATTGAGAAGAACT

TTGTCATTACTGACCCAAGATTGCCAGATAATCCCATTATATTCGCGTCCGATAGTTTCTTGCAGTTG
ACAGAATATAGCCGTGAAGAAATTTTGGGAAGAAACTGCAGGTTTCTACAAGGTCCTGAAACTGATC
GCGCGACAGTGAGAAAAATTAGAGATGCCATAGATAACCAAACAGAGGTCACTGTTCAGCTGATTAA
TTATACAAAGAGTGGTAAAAAGTTCTGGGCGCTCTTTCACTTGCAGCCTATGCG
AGATCAGAAGGGAGATGTCCAGTACTTTATTGGGGTTCAGTTGGATGGAACTGAGCATGTCCGAG
ATGCTGCCGAGAGAGAGGGAGTCATGCTGATTAAGAAAACTGCAGAAAATATTGATGAGGCGGCA
AAAGAACTTCTCGAGCTGCCGGAAACCGGTGGTGGTAGTGGTGGCTCTGGCGGTTCTGG
TGGCAGTGGCGGTAGCCAAGCTAAACCTCAAATTCCGAAAGATAAATCAAAAGTGGCAGGCTATATT
GAAATTCCAGATGCTGATATTAAAGAACCAGTATATCCAGGACCAGCAACACCTGAACAATTAAATAG
AGGTGTAAGCTTTGCAGAAGAAAATGAATCACTAGATGATCAAAATATTTCAATTGCAGGACACACTT
TCATTGACCGTCCGAACTATCAATTTACAAATCTTAAAGCAGCCAAAAAAGGTAGTATGGTGTACTTT
AAAGTTGGTAATGAAACACGTAAGTATAAAATGACAAGTATAAGAGATGTTAAGCCAACAGATGTAG
AAGTTCTAGATGAACAAAAAGGTAAAGATAAACAATTAACATTAATTACTTGTGATGATTACAATGAAA
AGACAGGCGTTTGGGAAAAACGTAAAATCTTTGTAGCTACAGAAGTCAAACATCACCACCATCATC
ACTAA

RS1-LOV2(N414D)-Jα-STEPL

ATGGGTAACGAAGCGTCTTACCCGCTGTTGGCTACTACACTTGAACGTATTGAGAAG
GATTTTGTCATTACTGACCCAAGATTGCCAGATAATCCCATTATATTCGCG
TCCGATAGTTTCTTGCAGTTGACAGAATATAGCCGTGAAGAAATTTTGGGAAGAAACTGCA
GGTTTCTACAAGGTCCTGAAACTGATCGCGCGACAGTGAGAAAAATTAGAGATGCCATAG
ATAACCAAACAGAGGTCACTGTTCAGCTGATTAATTATACAAAGAGTGGTAAAAAGTTCTG
GAACCTCTTTCACTTGCAGCCTATGCGAGATCAGAAGGGAGATGTCCAGTACTTTATTGG
GGTTCAGTTGGATGGAACTGAGCATGTCCGAGATGCTGCCGAGAGAGAGGGAGTCATGC
TGATTAAGAAAACTGCAGAAAATATTGATGAGGCGGCAAAAGAACTTCTCGAG CT
GCCGGAAACCGGTGGTGGTAGTGGTGGCTCTGGCGGTTCTGGTGGCAGTGGCGGT

AGCCAAGCTAAACCTCAAATTCCGAAAGATAAATCAAAAGTGGCAGGCTATATTGAAATT
CCAGATGCTGATATTAAAGAACCAGTATATCCAGGACCAGCAACACCTGAACAATTAAAT
AGAGGTGTAAGCTTTGCAGAAGAAAATGAATCACTAGATGATCAAAATATTTCAATTGCA
GGACACACTTTCATTGACCGTCCGAACTATCAATTTACAAATCTTAAAGCAGCCAAAAAA
GGTAGTATGGTGTACTTTAAAGTTGGTAATGAAACACGTAAGTATAAAATGACAAGTATAA
GAGATGTTAAGCCAACAGATGTAGAAGTTCTAGATGAACAAAAAGGTAAAGATAAACAAT
TAACATTAATTACTTGTGATGATTACAATGAAAAGACAGGCGTTTGGGAAAAACGTAAAA
TCTTTGTAGCTACAGAAGTCAAACATCACCACCATCATCACTAA

RS1-LOV2-KpnI-$(G_4S)_3$-BamHI-Jα-STEPL

ATGGGTAACGAAGCGTCTTACCCGCTGTTGGCTACTACACTTGAACGTATT
GAGAAGAACTTTGTCATTACTGACCCAAGATTGCCAGATAATCCCATTATATTCG
CGTCCGATAGTTTCTTGCAGTTGACAGAATATAGCCGTGAAGAAATTTTGGGAAG
AAACTGCAGGTTTCTACAAGGTCCTGAAACTGATCGCGCGACAGTGAGAAAAATT
AGAGATGCCATAGATAACCAAACAGAGGTCACTGTTCAGCTGATTAATTATACAAA
GAGTGGTAAAAAGTTCTGGAACCTCTTTCACTTGCAGCCTATGCGAGATCAGAAG
GGAGATGTCCAGTACTTTATTGGGGTTCAGTTGGATGGAACTGAGGGTACC
GGCGGAGGGGGTTCTGGAGGAGGCGGTTCGGGGGGCGGGGG
CTCGGGATCCCATGTCCGAGATGCTGCCGAGAGAGAGGGAGTCATGCTG
ATTAAGAAAACTGCAGAAAATATTGATGAGGCGGCAAAAGAACTTCTCGAGCTGCCGG
AAACCGGTGGTGGTAGTGGTGGCTCTGGCGGTTCTGGTGGCAGTGGCGGTAG
CCAAGCTAAACCTCAAATTCCGAAAGATAAATCAAAAGTGGCAGGCTATATTGAA
ATTCCAGATGCTGATATTAAAGAACCAGTATATCCAGGACCAGCAACACCTGAAC
AATTAAATAGAGGTGTAAGCTTTGCAGAAGAAAATGAATCACTAGATGATCAAAAT
ATTTCAATTGCAGGACACACTTTCATTGACCGTCCGAACTATCAATTTACAAATCT

TAAAGCAGCCAAAAAAGGTAGTATGGTGTACTTTAAAGTTGGTAATGAAACACGT
AAGTATAAAATGACAAGTATAAGAGATGTTAAGCCAACAGATGTAGAAGTTCTAGA
TGAACAAAAAGGTAAAGATAAACAATTAACATTAATTACTTGTGATGATTACAATGA
AAAGACAGGCGTTTGGGAAAAACGTAAAATCTTTGTAGCTACAGAAGTCAAACA
TCACCACCATCATCACTAA

References

[1] C. Frantz, K. M. Stewart, and V. M. Weaver, "The extracellular matrix at a glance," *Journal of Cell Science*, vol. 123, pp. 4195–4200, 2010.

[2] A. Kumar, J. K. Placone, and A. J. Engler, "Understanding the extracellular forces that determne cell fate and maintenance," *The Company of Biologists, Development*, vol. 144, pp. 4261–4270, 2017.

[3] J. S. Park, J. S. Chu, A. D. Tsou, R. Diop, Z. Tang, A. Wang, and S. Li, "The effect of matrix stiffness on the differentiation of mesenchymal stem cells in response to tgf-beta," *Biomaterials*, vol. 32, pp. 3921–3930, 2011.

[4] P. Gilbert, K. Havenstrite, K. Magnusson, A. Sacco, N. Leonardi, P. Kraft, N. Nguyen, S. Thrun, M. Lutolf, and H. Blau, "Substrate elasticity regulates skeletal muscle stem cell self-renewal in culture," *Science*, vol. 329, pp. 1078–1081, 2010.

[5] T. R. Cox and J. T. Erler, "Remodeling and homeostasis of the extracellular matrix: implications for fibrotic diseases and cancer," *Disease Models and Mechanisms*, vol. 4, pp. 163–178, 2011.

[6] S. R. Caliari and J. A. Burdick, "A practilca guide to hydrogels for cell culture," *Natural Methods*, vol. 13, pp. 405–414, 2016.

[7] C. A. DeForest and K. S. Anseth, "Advances in bioactive hydrogels to probe and direct cell fate," *Annual Review of Chemical and Biomolecular Engineering*, vol. 3, pp. 421–444, 2012.

[8] K. Uto, J. H. Tsui, C. A. DeForest, and D.-H. Kim, "Dynamically tunable cell culture platforms for tissue engineering and mechanobiology," *Progress in Polymer Science*, vol. 65, pp. 53–82, 2017.

[9] E. R. Ruskowitz and C. A. DeForest, "Photoresponsive biomaterials for targeted drug delivery and 4d cell culture," *Nature Reviews Materials*, vol. 3, no. 17087, 2018.

[10] Z. Zheng, J. Hu, H. Wang, J. Huang, Y. Yu, Q. Zhang, and Y. Cheng, "Dynamic softening or stiffeninf a supramolecular hydrogel by ultraviolet or near-infrared light," *Applied Materials and Interfaces*, vol. 9, pp. 24 511–24 517, 2017.

[11] A. M. Rosales, S. L. Vega, F. W. DelRio, J. A. Burdick, and K. S. Anseth, "Hydrogels with reversible mechanics to probe dynamic cell microenvironments," *Angewandte Chemie International Edition*, vol. 56, pp. 12 132–12 136, 2017.

[12] R. Yang and H. Liang, "Dynamic electro-regulation of the stiffness gradient hydrogels," *The Royal Society of Chemistry Advances*, vol. 8, pp. 6675–6679, 2018.

[13] H. Y. Yoshikawa, F. F. Rossetti, S. Kaufmann, T. Kaindl, J. Madsen, U. Engel, A. L. Lewis, S. P. Armes, and M. Tanaka, "Quantitative evaluation of mechanosensing of cells on dynamically tinable hydrogels," *Journal of the American Chemical Society*, vol. 113, pp. 1367–1374, 011.

[14] L. Tseng, P. Mather, and J. Henderson, "Shape-memory-actuated change in scaffold fiber alignment directs stem cell morphology," *Acta Biomaterialia*, vol. 9, pp. 8790–8801, 2013.

[15] L. Liu, J. A. Shadish, C. Arakawa, K. Shi, J. Davis, and C. A. DeForest, "Cyclic stiffness modulation of cell-laden protein-polymer hydrogels in response to user-specidied stimuli including light," *Advance Biosystems*, vol. 2, p. 1800240, 2018.

[16] J. M. Christie, "Phototropin blue-light receptors," *Annual Reviews of Plant Biology*, vol. 58, pp. 21–45, 2007.

[17] A. Möglich, X. Yang, R. A. Ayers, and K. Moffat, "Structure and function of plant photoreceptors," *Annual Revies of Plant Biology*, vol. 61, pp. 21–47, 2010.

[18] M. Xue and C. J. Jackson, "Extracellular matrix reorganization during wound healing and its impact on abnormal scarring," *Advances in Wound Care*, vol. 4, no. 3, pp. 119–136, 2015.

[19] R. G. Wells, "Tissue mechanics and fibrosis," *Biochimica et Biophysica Acta*, vol. 1832, no. 7, pp. 884–890, 2013.

[20] J. P. Zayner and T. R. Sosnick, "Factors that control the chemistry of the lov domain photocycle," *PLOS ONE*, vol. 9, pp. 1–9, 2014.

[21] A. S. Halavaty and K. Moffat, "N- and c-terminal flanking regions modulate light-induce signal transduction in the lov2 domain of the blue light sensor phtotropin 1 from avena sativa," *American Chemical Society Biochemistry*, vol. 46, no. 49, pp. 14 001–14 009, 2007.

[22] C. A. DeForest and D. A. Tirrell, "A photoreversible protein-patterning approach for guiding stem cell fate in three-dimensional gels," *Nature Materials*, vol. 14, pp. 523–531, 2015.

[23] S. H. Ho and D. A. Tirrell, "Chemoenzymatic labeling of proteins for imaging in bacterial cells," *Journal of the American Chemical Society*, vol. 138, pp. 15 098–15 101, 2016.

[24] R. Warden-Rothman, I. Caturegli, V. Popik, and A. Tsourkas, "Sortase-tag expressed protein ligation (STEPL): combining protein purification and site-specific bioconjugation into a single step," *Analytical Chemistry*, vol. 85, no. 22, pp. 2–22, 2013.

[25] J. A. Shadish, G. M. Benuska, and C. A. DeForest, "Bioactive site-specifically modified proteins for 4d patterning of gel biomaterials," *Nature Materials*, vol. In press, 2019.

[26] H.-Y. Liu, H. D. Nguyen, and C.-C. Lin, "Dynamic peg-peptide hydrogels via visible light ad fmn-induce tyrosine dimerization," *Advance Healthcare Materials*, vol. 7, pp. 1–10, 2018.